Virchows Arch (1995) 426:501–507

ORIGINAL ARTICLE

S.A. Zoubi · T.M. Mayhew · R.A. Sparrow

The small intestine in experimental diabetes: cellular adaptation in crypts and villi at different longitudinal sites

Received: 6 March 1995 / Accepted: 30 March 1995

Abstract Intestinal adaptation at the cellular level was examined in groups of streptozotocin-diabetic and age-matched control rats. Small intestines were removed and divided into four segments of roughly equal length. For each segment, epithelial volume, villous and microvillous surface areas and the mean volumes of epithelial cells in crypts and villi were estimated. From these data, we were able to estimate total numbers of epithelial cells in crypts and villi, assess adaptation at the level of the average cell and explore variation along the crypt-villus axis, between segments and between groups. Whilst the villus:crypt cell ratio did not change, diabetic animals contained about 80% more epithelial cells than control rats. The morphophenotype of villous epithelial cells (represented by nuclear volume, cell height, area and volume, and number and surface area of microvilli) was basically the same as that in controls. By contrast, crypt cells and their nuclei were 40–50% bigger in diabetic rats. Significant differences between segments were confined to the numbers and sizes of crypt cells and their nuclei. We conclude that experimental diabetes leads to both proliferative and hypertrophic responses within crypts. Crypt cells become fatter but not taller. Crypt hyperplasia is accompanied by an equiproportionate increase in villous epithelial cells, but these are of essentially normal morphophenotype.

Key words Intestinal villi · Crypts · Epithelial cells · Cell number · Cell size

Introduction

Streptozotocin-diabetic (STZD) rats display the symptoms of untreated diabetes, viz loss of body weight, high blood glucose levels, polyuria, glucosuria, polydipsia, hyperphagia and premature death. Their small intestines are heavier than those of normal rats, and this is associated with enhanced water and nutrient transport, changes in villous microvasculature and blood flow, deeper crypts and taller villi [10, 27–29, 31, 34, 47, 49, 56, 58, 59]. Since the number of villi per intestine seems to be fixed through much of normal life [11, 12, 18], the morphological responses imply that hyperplasia and/or hypertrophy contribute to transport changes. In fact, there is evidence for both phenomena.

In diabetes, as in other states, the intestine might adapt by altering one or more factors, viz cell number, activity and maturation along the vertical (crypt-villus) or longitudinal (pyloro-ileocolic) axes. Changes in cell morphology or apical transmembrane Na^+ gradients alone are likely to have non-specific effects on nutrient transport. However, changes in these three basic factors might influence specific transport processes, e.g. by allowing greater areas of plasma membrane in which to incorporate more of the same or different transport sites of the same or greater activity [28, 33].

Water content, DNA content and protein/DNA ratio are higher than normal in experimental diabetic intestines [46, 56]. There is also greater crypt activity with a decrease in villous turnover time [45]. Jejunal epithelial cells at villous tips are taller and villous sections contain more cell profiles [29, 58]. The changes may not affect all parts of the intestine equally; morphological, biochemical and kinetic studies point to a preferential effect at more distal sites [38, 45, 50, 58, 59].

In earlier investigations on STZD rats and their age-matched controls (AMC), we confirmed some of these structural changes. It was found that STZD animals were lighter than AMC rats with wider but not significantly longer small intestines. Absorptive surface areas and the volumes of crypts and villi were elevated but disproportionate and this led to changes in villous height and shape [38]. Unpublished results indicated that crypt mitotic figures increased and that crypt volume expanded by changes in diameter rather than in length. At the ultrastructural level, diabetes did not alter the mean length, diameter or packing density of microvilli [35, 61]. Con-

S.A. Zoubi · T.M. Mayhew (✉) · R.A. Sparrow
Department of Human Morphology, Queen's Medical Centre, University of Nottingham, Nottingham NG7 2UH, UK

sequently, changes in the absolute numbers and surface area of microvilli were commensurate with those in villous surface area, and this led us to suggest that the key adaptive response is an increase in epithelial cell number [35]. Support for the notion of a preferential effect in distal regions was also found [35, 38].

The present study directly addresses the degree of hyperplasia versus hypertrophy. It tests for the former by providing estimates of the numbers of crypt and villous epithelial cells [65] and for the latter by monitoring cell phenotypes in terms of volumes [65], surface areas and heights. Numbers and surface areas of microvilli per cell are also calculated and analyses of vertical and longitudinal gradients are included. The study provides a baseline not only for correlation with kinetic and transport data but also for assessing the efficacy of alternative forms of therapeutic intervention [41, 61].

Materials and methods

Animals

As part of a larger study [6, 38, 41, 61, 65], 20 male Sprague-Dawley rats (11 weeks old, 400–500 g body weight) were divided into two groups of equal size and roughly equal mean body weight (460 g). They were maintained on a 14 h-10 h light-dark cycle, fed a standard pellet diet and allowed ad libitum access to bottled drinking water. In one group (STZD group), diabetes was induced under ether anaesthesia by intraperitoneal injection of streptozotocin (median dosage 58 mg/kg body weight). Blood glucose levels rose to above 14 mmol/l within 2 days of injection. The other group comprised AMC animals. The present results are based on n=6 animals randomly selected (by lottery) from each of the AMC and STZD groups.

At the age of 23 weeks, animals were reweighed and killed under ether anaesthesia and at the same time of day so as to reduce the effects of diurnal variation. They were killed by intracardiac perfusion with an isotonic saline pre-wash followed by 2.5% glutaraldehyde in Millonig's phosphate buffer at room temperature (pH 7.3). After perfusion, the intestine was cut at the pylorus and the ileocolic junction, freed of mesentery and removed in toto. Its total length was measured.

Tissue sampling and microscopy

Procedures for light microscopical (LM) analyses are described in earlier reports [35, 38, 61]. Each intestine was cut transversely into four segments of roughly equal length (labelled A-D from duodenum to ileum). Each segment was sliced further into shorter pieces of which one was chosen at random. After flushing of the lumen with fresh fixative, each piece was trimmed. Following a buffer wash, the four pieces from each intestine were fixed secondarily for 2 h in 1% phosphate-buffered osmium tetroxide, dehydrated in graded ethanol concentrations and resin-embedded in flat moulds. Pieces were subsequently oriented on dummy resin blocks.

For LM, complete transverse semithin sections were cut and stained with toluidine blue. These were viewed as projected images at final linear magnifications (M) of M1=39–72 (low power) and M2=109 (high power) calibrated with external standards. Low-power sections were viewed entire but systematic random samples of fields [24], selected with the aid of the x,y scales on the microscope stage, were viewed at high power.

For transmission electron microscopy (TEM), the same blocks were trimmed [40] and ultrathin sections were cut and contrasted with lead citrate/uranyl acetate. They were mounted on copper support grids and examined at an accelerating voltage of 80 kV using a Philips EM300 microscope. At low power, epithelium was uniformly sampled as local vertical windows (full-depth sections normal to the surface) using grid squares as a sampling guide. Since epithelial cell nuclei approximate rotational ellipsoids whose major axes are aligned at right angles to the basal lamina, local vertical windows may be treated as vertical sections [5] for nuclear volume estimation. Sets of 3–4 fields per section were recorded and printed as photomontages at M3=5240 using carbon grating replicas as external calibration standards. Finally, further sets of 5–10 random fields showing the villous surface were sampled and printed at M4 = 22600.

Stereological analyses

On low-power LM projections, villous and crypt volumes per segment were obtained by multiplying cross-sectional areas (estimated by test point counting [36, 37, 60]) by segment length [39]. At the same magnification level, and in an analogous manner, villous surface areas were estimated by intersection counting [35, 39].

Epithelial volumes (crypts, villi) per segment were calculated from point counts made on high-power LM projections. In these estimates, and others, the term villous includes non-cryptal intervillous mucosa [65].

Intra-epithelial nuclear volume densities were estimated on TEM fields by point counting and volume-weighted mean nuclear volumes by measuring point-sampled intercept lengths [23]. Fields were analysed using test lattices of parallel straight lines superimposed at sine-weighted angles [5, 14, 23]. Multiplying nuclear volume density by epithelial volume provided the total volume of epithelial nuclei in each segment. Dividing this estimate by mean nuclear volume gave the number of epithelial nuclei in each segment [65]. Numbers of crypt and villous cells were estimated separately regardless of type (e.g. Paneth, enteroendocrine, goblet or absorptive epithelial cells).

Cell number estimates are biased because nuclear volume is volume- rather than number-weighted and the error is governed by the volume-frequency distribution of nuclei [14, 23]. Fortunately, epithelial nuclei are rather uniform in size and the bias is unimportant [16, 42]. Estimates also rely on two assumptions, viz (i) each epithelial cell has one nucleus and (ii) epithelium is wholly cellular. The former is justified but the latter introduces a small bias (up to 6% on villi but smaller in crypts) because intra-epithelial lymphocytes and basal extracellular spaces exist between epithelial cells.

Relative and absolute surface areas and numbers of microvilli on villous epithelial cells were estimated by intersection and profile counting methods [35, 61]. Segmental estimates of the lengths and diameters of microvilli were made using suitably sectioned organelles, and from these packing densities at the cell apex were calculated. Figures were corrected for overprojection effects using methods modified from those described by Gundersen [22].

Epithelial cell height was calculated by dividing volume by surface area. Dividing estimates of villous surface area by cell number gave a mean area which may be envisaged as that of the cell apex (unmodified by the presence of microvilli) or the cell base (the area of cell attachment to the basal lamina). The product of this area and cell height is equivalent to cell volume. From values of cell number and total microvillous surface and number, the surface area and number of microvilli per average villous epithelial cell were calculated.

Statistics

Estimates for each intestinal segment were expressed as group means and standard errors of means (SEM). They were also summed to obtain figures for the entire small intestine. Initially, apparent trends for variables to decline between segments were tested using Page's 'L' test [44] with k=4 segments and n=6 rats.

Table 1 Cell number and morphophenotype in crypt epithelium of diabetic (STZD) and control (AMC) rats. Values are group means (SEM)

Variable	Segment A	Segment B	Segment C	Segment D
Cell number ($\times 10^9$)				
AMC	0.52 (0.14)	0.89 (0.07)	1.25 (0.31)	0.66 (0.18)
STZD	1.02 (0.19)	1.40 (0.30)	1.88 (0.42)	1.62 (0.39)
Cell height (μm)				
AMC	20 (0.8)	20 (0.9)	21 (0.8)	20 (1.0)
STZD	22 (0.6)	21 (1.4)	21 (0.9)	20 (0.3)
Nuclear volume (μm^3)				
AMC	81 (9.6)	75 (7.3)	44 (5.6)	58 (6.0)
STZD	121 (26.5)	83 (7.3)	94 (22.9)	70 (8.9)
Cell volume (μm^3)				
AMC	386 (40)	233 (32)	166 (31)	220 (28)
STZD	447 (94)	349 (54)	354 (87)	272 (46)
Cell surface without microvilli (μm^2)				
AMC	19.6 (2.7)	11.5 (1.8)	7.6 (1.2)	11.8 (1.8)
STZD	19.9 (3.6)	17.5 (2.7)	17.1 (3.8)	13.5 (2.3)

Table 2 Cell number and morphophenotype in villous epithelium of diabetic (STZD) and control (AMC) rats. Values are group means (SEM)

Variable	Segment A	Segment B	Segment C	Segment D
Cell number ($\times 10^9$)				
AMC	0.98 (0.10)	1.98 (0.30)	1.09 (0.10)	1.04 (0.30)
STZD	2.02 (0.39)	2.51 (0.64)	2.66 (0.52)	1.95 (0.56)
Cell height (μm)				
AMC	31 (1.9)	29 (2.1)	27 (3.0)	23 (2.5)
STZD	29 (1.9)	27 (2.6)	30 (2.3)	25 (2.6)
Nuclear volume (μm^3)				
AMC	103 (6.1)	66 (7.6)	67 (4.8)	62 (17.2)
STZD	77 (5.0)	77 (11.1)	68 (6.8)	94 (16.2)
Cell volume (μm^3)				
AMC	525 (52)	335 (36)	337 (41)	331 (78)
STZD	459 (58)	456 (62)	429 (51)	498 (90)
Cell surface (μm^2)				
Without microvilli				
AMC	18.0 (1.5)	12.7 (1.9)	14.9 (1.7)	15.6 (2.3)
STZD	15.8 (1.6)	17.7 (3.1)	14.7 (1.9)	20.0 (3.0)
With microvilli				
AMC	178 (27)	210 (34)	271 (35)	174 (26)
STZD	165 (23)	227 (33)	227 (41)	263 (66)
Microvilli per cell				
AMC	557 (46)	456 (67)	628 (72)	462 (68)
STZD	476 (49)	638 (112)	543 (70)	721 (107)

Differences between groups and segments were examined further using two-way analyses of variance [57]. The null hypothesis (that there is no difference between groups or between segments) was rejected if the P value was less than 0.05 for the appropriate degrees of freedom.

Results

Segmental differences (Tables 1, 2)

For control rats, Page's tests revealed significant regional trends for all variables except the numbers and surface areas of microvilli per villous epithelial cell. Segmental trends in crypt cell number, volume, area and height disappeared in STZD rats, as did the variation in nuclear volume, cell volume, area and height of villous cells.

Vertical differences (Tables 1–3)

With progression along the crypt-villus axis, there were marked changes in epithelial cell morphology. In both groups, cells became taller (30–33% overall) and more voluminous (46–74%), but only in AMC rats did they become consistently fatter (38%). Thus, cells in AMC rats grew by a combination of increases in height and girth, whilst those in STZD rats grew mainly by becoming taller. Indeed, in some segments, STZD cells became thinner as they made the crypt-villus transition.

Effects of experimental diabetes (Tables 1–3)

In the main, two-way analyses of variance supported the regional differences identified above and did not reveal

Table 3 Cell number and morphophenotype in villous and crypt epithelia in diabetic (STZD) and control (AMC) rats. Values are group means (SEM) for the entire intestine. Results for group mean comparisons are based on 2-way analyses of variance with 1,40 *df* (*NS* not significant)

Variable	AMC rats	STZD rats	Apparent change	P level
Cell number ($\times 10^9$)				
Crypts	3.32 (0.32)	5.91 (0.77)	78%	**
Villi	5.10 (0.62)	9.14 (1.53)	79%	***
Cell height (μm)				
Crypts	20 (0.5)	21 (0.5)	5%	NS
Villi	26 (1.6)	28 (1.3)	8%	NS
Nuclear volume (μm^3)				
Crypts	56 (2.9)	82 (10.0)	46%	**
Villi	71 (7.6)	74 (5.2)	4%	NS
Cell volume (μm^3)				
Crypts	207 (17.5)	304 (37.9)	47%	*
Villi	360 (40.6)	444 (45.8)	23%	NS
Cell surface (μm^2)				
Without microvilli				
Crypts	10.3 (0.98)	14.8 (1.60)	44%	*
Villi	14.2 (1.31)	16.0 (1.83)	13%	NS
With microvilli				
Villi	202 (22.7)	214 (25.1)	6%	NS
Microvilli per cell				
Villi	493 (45.7)	560 (66.0)	14%	NS

* $P<0.05$; ** $P<0.01$; *** $P<0.001$

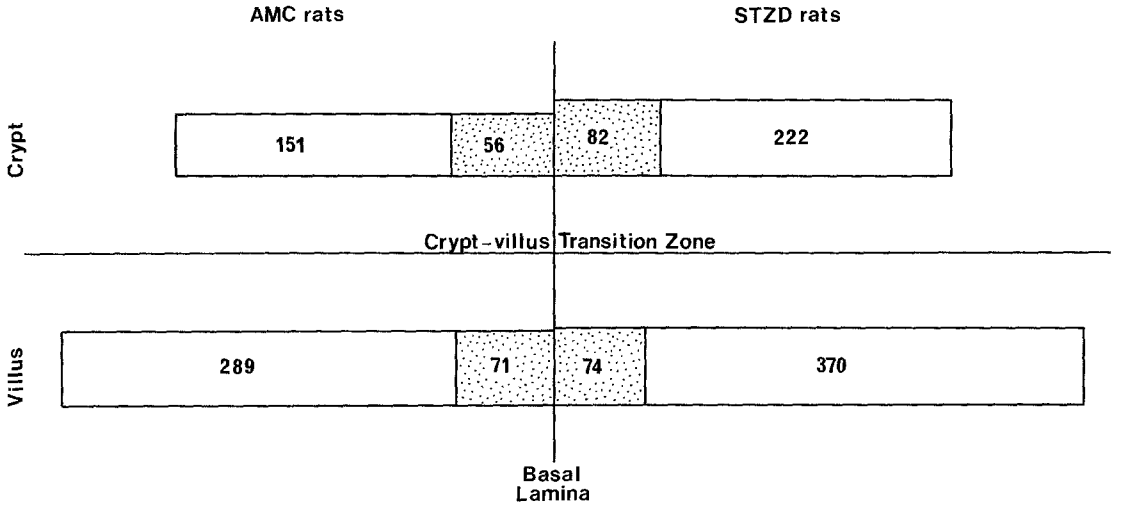

Fig. 1 The principal differences between the average cells (in crypts and on villi) in the small intestines of age-matched control (*AMC*) and streptozotocin-diabetic (*STZD*) rats. Each cell is represented by a *rectangle* whose length is proportional to cell height and whose width is proportional to the square root of apex area. Within each *rectangle*, the *numbers* are the mean volumes (μm^3) for the nucleus (*stippled*) and cytoplasm (*plain*). In passing from crypt to villus, cell size increases in both groups of rats. In crypts of STZD rats, cell apex area, cell volume and nuclear volume are greater than in AMC rats. Villous epithelial cells in STZD rats are not significantly different from those in AMC animals

any significant interaction effects. As for crypts, the principal differences between AMC and STZD groups were in nuclear volume, cell number, cell volume and apex area. Apparent differences in mean cell height were not significant. In the case of villi, there was an increase in cell number in diabetics but cell morphophenotype did not alter.

Values per intestine (Table 3, Fig. 1)

AMC rats harboured 3.3×10^9 crypt epithelial cells and 5.1×10^9 villous epithelial cells. Both numbers increased 1.8-fold in STZD animals, so that the villus:crypt cell ratio was maintained. Crypt hyperplasia was accompanied by changes in cell morphophenotype. In particular, both nuclear and cell volumes rose by roughly 46%. Since cell height did not alter significantly, cell growth can be attributed to crypt cell fattening (apex area increased 44%, from approximately 10 μm^2 to 15 μm^2). In contrast, there was no detectable change in the morphology of villous cells as assessed in terms of volume, height, apex area, microvillous area, microvillous number and nuclear volume.

Discussion

This study has focused on epithelial cell morphophenotype and number in the crypts and villi of normal and diabetic small intestine. In 12-week STZD rats, the adaptive response of crypts was both hyperplastic and hypertrophic. Crypt cell number increased by almost 80% and mean cell volume by less than 50%. In contrast, the villous response was due purely to nett cell recruitment, villi harbouring 80% more cells of essentially normal morphophenotype. As in an earlier study on control animals [65], no evidence for the numerical equivalence of crypt and villous cells was found. In both AMC and STZD animals, there were 55% more villous cells than crypt cells and villous cells were predominant all along the intestine. In making the crypt-villus transition, the average cell became taller and more voluminous but, at least in STZD animals, not fatter.

Vertical differentiation and longitudinal variation

Our evidence for an increase in the height, volume and apex area of epithelial cells in passing from crypt to villous compartments reinforces results obtained elsewhere. However, it may underestimate the magnitude of the differences involved because it is based on the average crypt cell and average villous cell. It is known that the ultrastructural phenotype of columnar absorptive epithelial cells develops gradually as cells migrate from the base of the crypt, through the proliferative zone and to the functional zone. Within this zone, crypt cells no longer divide but mature more rapidly [15]. Only at the crypt-villus junction do marked increases occur in nuclear size, cell size and organelle content or size (including Golgi, smooth and rough ER membranes, mitochondria and microvilli). Thereafter maturation continues as cells migrate towards the villous tip [1, 3, 8, 15, 32, 43, 52, 53, 54]. Biochemical analysis of brush border enzymes indicates that their activities parallel the structural development of microvilli, though not faithfully [7, 8, 19, 48].

Our findings are also consistent with the proximodistal gradients of villous morphology and activity seen in normal animals. More proximal segments are of greater import for nutrient digestion and transport, tend to have more cells and show greater absorptive surface areas. They also have higher villus:crypt cell ratios [4, 28, 35, 39, 62, 65].

Effects of experimental diabetes

The populations of intestinal villi and crypts are relatively fixed through the lifespan of the rat, there being about 140,000 villi and 18 crypts per villus on average [11–13, 18]. Assuming that these figures hold for the present animals, the epithelial cell populations found here represent about 36,000 cells per villus in AMC and 65,000 per villus in STZD rats. Corresponding figures for cells per crypt would be 1300 (AMC group) and 2300 (STZD group). Thus, cell complements on villi and crypts are almost doubled after diabetes of 12 weeks' duration. This level of change, coupled with a stable cell morphophenotype, can easily account for the increase in villous height, the change of villous shape and the doubling of villous and microvillous surface areas revealed in earlier studies [35, 38]. They also help to account for the observed increases in the absorption of glucose and other nutrients [28]. The increases in crypt cell volume could also account for the greater crypt volume and diameter.

The reasons for changes in crypt cell size and nuclear volume are unclear. However, it seems that crypt and villous cells are limited in their linear growth, since heights did not alter during diabetes. It may be that there are constraints imposed by local tissue architecture (e.g. spatial packing of crypts and villi) or by functional disadvantages consequent upon them (e.g. the impact on nutrient transport of unstirred layer effects [28, 33]. Experimental diabetes can alter chromatin structure in nuclei from cells in brain, liver and intestinal epithelium [25] but the biological significance of these changes is unknown.

The signals responsible for elevated nutrient absorption in diabetes are unclear. Candidates include insulin deficiency, high blood glucose and high intracellular glucose in epithelial cells [28]. Insulin affects the activities of brush border enzymes [63], and there is evidence for the presence of insulin and insulin-like growth factor (IGF) binding sites on epithelial cells [17, 20, 26, 30, 51]. Although it has also been suggested that insulin exerts a general trophic effect on DNA synthesis, recent evidence indicates that it does not have a major role in the regulation of cell proliferation [21] and so the hyperplasia of diabetes may be a consequence of hyperphagia. The expression of IGF receptors on crypt cells may indicate a role in the control of cell growth but, unfortunately, little is known about their incidence, activity or regulation in diabetes.

Various growth factors play important roles in intestinal epithelial renewal, including transforming growth factor-α, epidermal growth factor, trefoil peptides and enteroglucagon [2]. Potten et al. [55] have extracted a potent stimulator (a small protein or peptide) of intestinal cell proliferation from small intestine subjected to irradiation. Recent studies on isolated intestinal epithelial cells have suggested that the hyperplasia of STZ-induced diabetes is associated with increased activity of ornithine decarboxylase and increased contents of polyamines, notably putrescine and spermidine [64]. Administration of difluoro-α-methylornithine (an ornithine decarboxylase inhibitor) reduced or prevented hyperplasia in STZD-rats and retarded epithelial growth in control rats.

Intestinal epithelial cells absorb monosaccharides by energy-dependent and energy-independent mechanisms. Na^+-dependent glucose transporter 1 (SGLT1) initiates glucose absorption and is located in the microvillous membrane. Efflux occurs at basolateral membranes via a product (GLUT2) of the family of facilitative glucose

transporter genes. In STZD-rats, the increase in total hexose transport is associated with early expression of transporters by epithelial cells on the crypt-villus axis [9]. The finding that microvilli on villous epithelial cells are unaltered structurally in STZ-diabetes suggests that early expression may be due to early incorporation of SGLT1 protein or to structural modifications rendering it more active. As yet, there are no parallel morphometric data on basolateral membranes.

Acknowledgements We wish to thank the Ministry of Higher Education (Libya) for supporting S.A.Z. and Messrs Alan Pyper, Tim Self and Barry Shaw for expert technical assistance.

References

1. Abbas B, Hayes TL, Wilson DJ, Carr KE (1989) Internal structure of the intestinal villus: morphological and morphometric observations at different levels of the mouse villus. J Anat 162: 263–273
2. Alison MR, Sarraf CE (1994) The role of growth factors in gastrointestinal cell proliferation. Cell Biol Int 18: 1–10
3. Altmann GG (1990) Renewal of the intestinal epithelium: new aspects as indicated by recent ultrastructural observations. J Electron Microsc Techn 16: 2–14
4. Altmann GG, Enesco M (1967) Cell number as a measure of distribution and renewal of epithelial cells in the intestine of growing and adult rats. Am J Anat 121: 319–336
5. Baddeley AJ, Gundersen HJG, Cruz-Orive L-M (1986) Estimation of surface area from vertical sections. J Microsc 142: 259–276
6. Bhoyrul S, Sharma AK, Stribling D, Mirrlees DD, Peterson RG, Farber MO, Thomas PK (1988) Ultrastructural observations on myelinated fibres in experimental diabetes: effect of the aldose reductase inhibitor Ponalrestat given alone or in conjunction with insulin therapy. J Neurol Sci 85: 131–147
7. Both NJ de, Dongen JM van, Hofwegen B van, Keulemans J, Visser WJ, Galjaardt H (1974) The influence of various cell kinetic conditions on functional differentiation in the small intestine of the rat. A study of enzymes bound to sub-cellular organelles. Dev Biol 38: 119–137
8. Brown AL (1962) Microvilli of the human jejunal epithelial cell. J Cell Biol 12: 623–627
9. Burant CF, Flink S, DePaoli AM, Chen J, Lee W-S, Hediger MA, Buse JB, Chang EB (1994) Small intestine hexose transport in experimental diabetes. J Clin Invest 93: 578–585
10. Caspary WF (1973) Effect of insulin and experimental diabetes mellitus on the digestive absorptive function of the small intestine. Digestion 9: 248–263
11. Clarke RM (1970) Mucosal architecture and epithelial cell production rate in the small intestine of the albino rat. J Anat 107: 519–529
12. Clarke RM (1972) The effect of growth and fasting on the number of villi and crypts in the small intestine of the albino rat. J Anat 112: 27–33
13. Clarke RM (1977) The effects of age on mucosal morphology and epithelial cell production in rat small intestine. J Anat 123: 805–811
14. Cruz-Orive L-M, Hunzicker EB (1986) Stereology for anisotropic cells: application to growth cartilage. J Microsc 143: 47–80
15. Dongen JM van, Visser WJ, Daems WT, Galjaard H (1976) The relation between cell proliferation, differentiation and ultrastructural development in rat intestinal epithelium. Cell Tissue Res 174: 183–199
16. Elbrønd VS, Dantzer V, Mayhew TM, Skadhauge E (1991) Avian lower intestine adapts to dietary salt (NaCl) depletion by increasing transepithelial sodium transport and microvillous membrane surface area. Exp Physiol 76: 733–744
17. Forgue-Lafitte ME, Marescot MR, Chamblier MC, Rosselin G (1980) Evidence for the presence of insulin binding sites in isolated rat intestinal epithelial cells. Diabetologia 19: 373–378
18. Forrester JM (1972) The number of villi in rat's jejunum and ileum: effect of normal growth, partial enterectomy and tube feeding. J Anat 111: 283–291
19. Galjaard H, Meer-Flieggen W van der, Both NJ de (1972) Cell differentiation in gut epithelium. In: Viza D, Harris H (eds) Cell differentiation. Munksgaard, Copenhagen, pp 322–328
20. Gallo-Payet N, Hugon JS (1984) Insulin receptors in isolated adult mouse intestinal cells: studies in vivo and in organ culture. Endocrinology 114: 1885–1892
21. Goodlad RA, Lee CY, Gilbey SG, Ghatei MA, Bloom SR (1993) Insulin and intestinal epithelial cell proliferation. Exp Physiol 78: 697–705
22. Gundersen HJG (1979) Estimation of tubule or cylinder L_v, S_v and V_v on thick sections. J Microsc 117: 333–345
23. Gundersen HJG, Jensen EB (1985) Stereological estimation of the volume-weighted mean volume of arbitrary particles observed on random sections. J Microsc 138: 127–142
24. Gundersen HJG, Jensen EB (1987) The efficiency of systematic sampling and its prediction. J Microsc 147: 229–263
25. Hartnell JM, Storrie MC, Mooradian AD (1990) Diabetes-related changes in chromatin structure of brain, liver, and intestinal epithelium. Diabetes 39: 348–353
26. Heinz-Erian P, Kessler U, Funk B, Gais P, Kiess W (1991) Identification and in situ localisation of the insulin-like growth factor II/mannose-6-phosphate (IGF-II/M6P) receptor in the rat gastrointestinal tract: comparison with the IGF-I receptor. Endocrinology 129: 1769–1778
27. Jervis EL, Levin RJ (1966) Anatomic adaptation of the alimentary tract of the rat to the hyperphagia of chronic alloxan-diabetes. Nature 210: 391–393
28. Karasov WH, Diamond JM (1983) Adaptive regulation of sugar and amino acid transport by vertebrate intestine. Am J Physiol 245: G443-G462
29. Keelan M, Walker K, Thompson ABR (1985) Intestinal brush border membrane marker enzymes, lipid composition and villus morphology: effect of fasting and diabetes mellitus in rats. Comp Biochem Physiol 82A: 83–89
30. Laburthe M, Rouyer F, Gammeltoft S (1988) Receptors for insulin-like growth factors I and II in rat gastrointestinal epithelium. Am J Physiol 245: G457-G462
31. Lal D, Schedl HP (1974) Intestinal adaptation in diabetes: amino acid absorption. Am J Physiol 227: 827–831
32. Leblond CP (1981) The life history of cells in renewing systems. Am J Anat 160: 114–158
33. Levin RJ (1984) Intestinal adaptation to dietary change as exemplified by dietary restriction studies. In: Batt RM, Lawrence TLJ (eds) Function and dysfunction of the small intestine. Liverpool University Press, Liverpool, pp 77–93
34. Lorenz-Meyer H, Gottesburen H, Menge H, Bloch R, Riecken EO (1974) Intestinal structure and function in relation to blood sugar levels and food intake in experimental diabetes. In: Dowling RH, Riecken EO (eds) Intestinal adaptation. Schattauer, Stuttgart, pp 189–191
35. Mayhew TM (1990) Striated brush border of intestinal absorptive epithelial cells: stereological studies on microvillous morphology in different adaptive states. J Electron Microsc Techn 16: 45–55
36. Mayhew TM (1991) The new stereological methods for interpreting functional morphology from slices of cells and organs. Exp Physiol 76: 639–665
37. Mayhew TM (1992) A review of recent advances in stereology for quantifying neural structure. J Neurocytol 21: 313–328
38. Mayhew TM, Carson FL (1989) Mechanisms of adaptation in rat small intestine: regional differences in quantitative morphology during normal growth and experimental hypertrophy. J Anat 164: 189–200
39. Mayhew TM, Middleton C (1985) Crypts, villi and microvilli in the small intestine of the rat. A stereological study of their variability within and between animals. J Anat 141: 1–17

40. Mayhew TM, Middleton C, Ross GA (1988) Dealing with oriented surfaces: studies on villi and microvilli of rat small intestine. In: Reith A, Mayhew TM (eds) Stereology and morphometry in electron microscopy. Problems and solutions. Hemisphere, New York, pp 85–98
41. Mayhew TM, Carson FL, Sharma AK (1989) Small intestinal morphology in experimental diabetic rats: a stereological study on the effects of an aldose reductase inhibitor (ponalrestat) given with or without conventional insulin therapy. Diabetologia 32: 649–654
42. Mayhew TM, Elbrønd VS, Dantzer V, Skadhauge E, Moller O (1992) Structural and enzymatic studies on the plasma membrane domains and sodium pump enzymes of absorptive epithelial cells in the avian lower intestine. Cell Tissue Res 270: 577–585
43. McElligott TF, Beck IT, Dinda PK, Thompson S (1975) Correlation of structural changes at different levels of the jejunal villus with positive and negative net water transport in vivo and in vitro. Can J Physiol Pharmacol 53: 439–450
44. Miller DL, Hanson W, Schedl HP, Osborne JW (1977) Proliferation rate and transit time of mucosal cells in the small intestine of the diabetic rat. Gastroenterology 73: 1326–1332
45. Miller S (1975) Experimental design and statistics. Methuen, London
46. Nakabou Y, Okita C, Takano Y, Hagiira H (1974) Hyperplastic and hypertrophic changes of the small intestine. J Nutr Sci Vitaminol 20: 227–234
47. Nakabou Y, Ishikawa Y, Misaki A, Hagihira H (1980) Effect of food intake on intestinal absorption and hydrolases in alloxan-diabetic rats. Metabolism 29: 181–185
48. Nordstrom C, Dahlqvist A, Josefsson L (1968) Quantitative determination of enzymes in different parts of the villi and crypts of rat small intestine. J Histochem Cytochem 15: 713–721
49. Olsen WA, Rosenberg IH (1970) Intestinal transport of sugars and amino acids in diabetic rats. J Clin Invest 49: 96–105
50. Olsen W, Agresti HL, Lorentzsonn VW (1974) Intestinal disaccharidases in diabetic rats. In: Dowling RH, Riecken EO (eds) Intestinal adaptation. Schattauer, Stuttgart, pp 179–187
51. Park JH, Vanderhoof JA, Blackwood D, MacDonald RG (1990) Characterisation of type I and type II insulin-like growth factor receptors in an intestinal epithelial cell line. Endocrinology 126: 2998–3005
52. Pothier P, Hugon JS (1980) Characterization of isolated villus and crypt cells from the small intestine of the adult mouse. Cell Tissue Res 211: 405–418
53. Potten CS (1980) Stem cells in small-intestinal crypts. In: Appleton DR, Sunter JP, Watson AJ (eds) Cell proliferation in the gastrointestinal tract. Pitman Medical, London, pp 141–154
54. Potten CS, Loeffler M (1987) A comprehensive model of the crypts of the small intestine of the mouse provides insights into the mechanisms of cell migration and the proliferation hierarchy. J Theor Biol 127: 381–391
55. Potten CS, Booth C, Chadwick CA, Evans GS (1994) A potent stimulator of small intestinal cell proliferation extracted by simple diffusion from intact irradiated intestine: in vitro studies. Growth Factors 10: 53–61
56. Schedl HP, Wilson HD (1971) Effects of diabetes on intestinal growth and hexose transport in the rat. Am J Physiol 220: 1739–1745
57. Sokal RR, Rohlf FJ (1981) Biometry. The principles and practice of statistics in biological research. Freeman, San Francisco
58. Stenling R, Hagg E, Falkmer S (1984) Stereological studies on the rat small intestinal epithelium. III. Effects of short-term alloxan diabetes. Virchows Arch [B] 47: 263–270
59. Tahara T, Yamamoto T (1988) Morphological changes of the villous microvascular architecture and intestinal growth in rats with streptozotocin-induced diabetes. Virchows Archiv [A] 413, 151–158
60. Weibel ER (1979) Stereological methods, vol 1: Practical Methods for Biological Morphometry. Academic Press, London
61. Williams M, Mayhew TM (1992) Responses of enterocyte micro-villi in experimental diabetes to insulin and an aldose reductase inhibitor (ponalrestat). Virchows Arch [B] 62: 385–389
62. Wright (1980) Cell proliferation in the normal gastrointestinal tract. Implications for proliferative responses. In: Appleton DR, Sunter JP, Watson AJ (eds) Cell proliferation in the gastrointestinal tract. Pitman Medical, London, pp 3–25
63. Younoszai MK, Parekh VV, Hoffman JL (1993) Polyamines and intestinal epithelial hyperplasia in streptozotocin-diabetic rats. Proceedings of the Society for Experimental Biology and Medicine 202: 206–211
64. Young GP, Morton CL, Rose IS, Taranto TM, Bhathal PS (1987) Effects of intestinal adaptation on insulin binding to villus cell membranes. Gut 28: 57–62
65. Zoubi SA, Mayhew TM, Sparrow RA (1994) Crypt and villous epithelial cells in adult rat small intestine: numerical and volumetric variation along longitudinal and vertical axes. Epithelial Cell Biol 3: 112–118